Journal of Engineering Science and Technology
Vol. 14, No. 1 (2019) 351 - 369

A MODIFIED MULTILEVEL INVERTER TOPOLOGY WITH MAXIMUM POWER POINT TRACKING FOR PHOTOVOLTAIC SYSTEMS

K. CHERIFI*, Y. MILOUD, M. MOSTEFAI

Electrotechnical Engineering Laboratory, Faculty of Technology,
Tahar Moulay University of Saida, BP 138, En-Nasr, Saida 20000, Algeria
*Corresponding Author: khaled.chirifi@gmail.com

Abstract

In this paper, both topologies, three level neutral-point clamped diode and the modified inverter are presented which are fed by PV system as DC source input to drive an induction motor. A fuzzy logic maximum power point tracking (MPTT) technique is used to ensure the PV array to operate at maximum power and to adjust the DC voltage. Simulation results show the feasibility and ability of the modified topology, which can improve the quality of power.

Keywords: Fuzzy logic controller, MPPT boost converter, Photovoltaic system, Three level inverter, Total harmonic distortion.

1. Introduction

The world went to alternative energy sources such as energy photovoltaic because it is available, clean and environmentally friendly energy [1].The extraction of energy from the PV module depends on the climatic conditions. This system has an optimum operating point called Maximum Power Point (MPP), which is largely dependent on the intensity of illumination. The adaptation of PV panels to the load is necessary to extract the maximum power of the PV module. This is done through a boost converter that controls the maximum power using a fuzzy logic controller. [2, 3].

An inverter is used to drive the induction motor with the maximum power extracted from the photovoltaic generator. The output voltage and frequency could be fixed. In various applications, it is often necessary to control the output voltage of the inverter [4].

Multilevel inverters are generally used for high power and high voltage applications. There are numerous advantages for multilevel inverters over conventional two level inverters [5].The principal characteristic of a multilevel inverter is its ability to operate at multiple small voltage levels to perform power conversion and to reduce the harmonic content of the output voltage. By using multilevel inverters instead of two level inverters, filters become smaller and cheaper. [6-8].

In order to attain a good performance of the inverter for a low total harmonic distortion (THD), there are several inverter topologies, which are, suggested in recent years, such as neutral-point clamped and flying-capacitor, cascaded-inverters and other hybrid [9].

Diode-clamped multilevel inverter (NPC) is the most utilized topology in the industry for high voltage applications. The most advantages of theses inverters are those having a high enough levels, the need for filtering is decreased since the harmonic contents will be low. However, a high number of levels has the disadvantage of requiring excessive clamping diodes that makes the power flow more difficult to control [10].

The proposed inverter is more efficient with low harmonic content, so the output waveform approaches the sine wave without needing the increase of the number of inverter levels. The feasibility of the modified topology is verified through the simulation and however, a comparison with conventional diode clamped inverter is made.

This paper is structured as follow: the explanation of the full system is presented in section two. In section three, a brief presentation and modelling of solar generator is made. Section four, describes the fuzzy logic MPPT controller with boost converter used to track the maximum power from PV Module. The modified structure and operation of three level inverter are given in section five. Presentation of control technique for three level inverter in section six, Simulation results and discussions are presented in section seven. Finally, this paper is ended by a conclusion.

2. System Description

The system studied is shown in Fig. 1. It consists of the PV array, the DC- DC boost converter, and two different three level inverter topologies. The DC- DC converter is controlled by a pulse width modulation signal with a maximum power point

tracking (MPPT) based on fuzzy logic. The three-level inverter fed by boost converter will supply the AC motor.

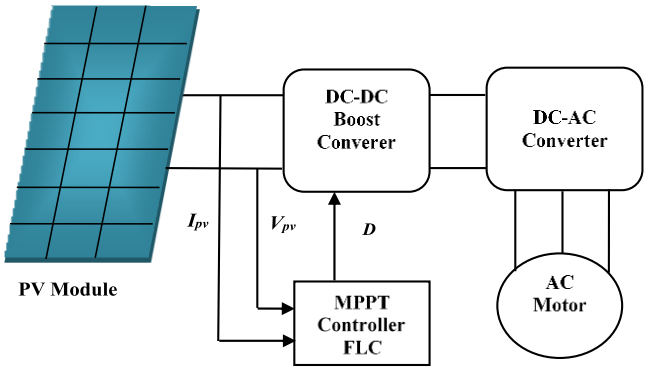

Fig. 1. Block diagram of the full system.

3. Mathematical Model for a Photovoltaic Module

The solar cell is the basic unit of photovoltaic generator, which transforms the sun's light directly into electricity. The equivalent circuit of PV cell is shown in Fig. 2 [11].

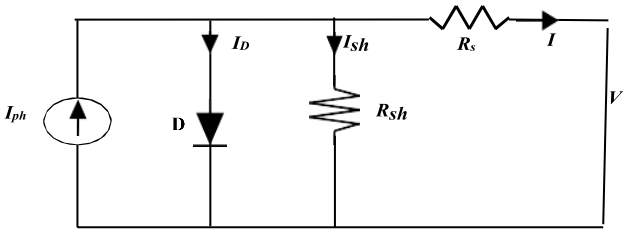

Fig. 2. PV cell equivalent circuit [11].

Equations (1) to (5) controlling the output current of PV module are as follow [11, 12]:

$$I = I_{ph} - I_d - I_{sh} \tag{1}$$

$$I_{ph} = \frac{G}{G_{ref}}(I_{ph,ref} + \mu_{icc} * \Delta T) \tag{2}$$

$$I_d = I_o.[\exp(\frac{V + R_s.I}{nV_T}) - 1] \tag{3}$$

$$I_{sh} = \frac{V + R_s.I}{R_{sh}} \tag{4}$$

$$I = I_{ph} - I_o.[\exp(\frac{V + R_s.I}{nV_T}) - 1] - \frac{V + R_s.I}{R_{sh}} \tag{5}$$

$$V_T = \frac{K.T}{q} \tag{6}$$

where G: irradiance, T: temperature condition of work, G_{ref}: irradiance at standard test conditions (STC), 1000 W/m^2 and 25°C, U_{icc}: temperature coefficient of current, I: the photovoltaic output current, q:theelectroncharge (1.60217646×10^{-19} C), k: Boltzmann constant (1.3806503×10^{-23} J/K), I_{ph}: light generated current in a PV module (A), I_o: diode saturation current, V: terminal voltage, R_s: series resistance of a PV module, R_{sh} : intrinsic shunt resistance of the cell, V_T: thermal voltage; n: ideality factor temperature.

The polycrystalline PV model (HA- 125-12) type of has been chosen, which consists of 36 cells with a power of 125 W. Table 1 summarizes the characteristics of this PV module.

Table 1. Electrical characteristics of the photovoltaic module "HA- 125-12".

Characteristics	Value
Rated Power	125 W
Open circuit voltage, V_{oc}	21.6 V
Short circuit current, I_{SC}	8.05 A
Voltage at Maximum power, V_m	17.25 V
Current at Maximum power, I_m	7.25 A

The power generation system is composed of 20 modules in series and 10 in parallel to form a power PV generator of 25 kW.

4. Boost Converter and MPPT Fuzzy Logic Controller

4.1. Boost Converter

DC-DC boost converter is a converter used to amplify the DC output voltage. As shown in Fig. 3, an input and output filters composed of inductance and capacitor respectively are used to reduce the ripple in current and a diode is used to prevent discharge in the source [13].

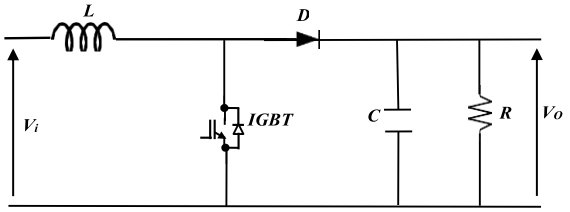

Fig. 3. Boost converter.

The output voltage (V_o) and duty cycle (D) are given by the following equations [14]:

$$V_o = \frac{V_i}{1-D} \tag{7}$$

So,

$$D = 1-\frac{V_i}{V_o} \tag{8}$$

Assuming a lossless circuit,

$$V_i.I_i = V_o.I_o = \frac{I_o.V_i}{1-D} \tag{9}$$

Then, the average output current is:

$$I_o = I_i(1-D) \tag{10}$$

The relations of the input and output filters (L) and (C) respectively are given by the following equations [15]:

$$L = \frac{D(1-D)^2 R}{2f} \tag{11}$$

$$C = \frac{D}{2fR} \tag{12}$$

Hence, the boost converter design values are shown in Table 2.

Table 2. Boost converter design values.

Parameters	Values
Input voltage, V_i	345V
Output voltage, V_o	600 V
Switching frequency, f	4 kHz
Duty cycle, D	0.425
Inductor, L	0.281mH
Capacitor, C	3.32 μF

4.2. MPPT fuzzy logic controller

Maximum power point tracking techniques contribute significantly to PV system performances. The idea behind MPPT is to continuously adjust the PV output power to its maximum value, which is mostly related to the changes in atmospheric conditions. A look at the literature reveals that there are different types of MPPT algorithms that can be used [16].

In this paper, MPPT fuzzy logic controller is used for boost converter. Compared with other algorithms (P&O), the fuzzy logic controller gives good tracking performance and its design is more or less simple.

As it is shown in Fig.4, the Fuzzy logic controller usually consists of three stages: fuzzification, fuzzy rules and defuzzification [17].

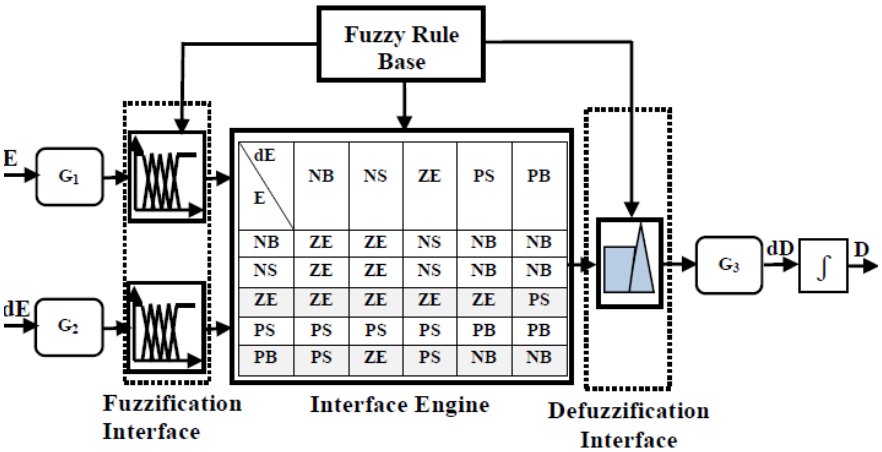

Fig. 4. Basic structure of a fuzzy logic controller.

The fuzzy logic controller inputs are the error E and change of error dE, which are calculated as:

$$E(K) = \frac{P_{pv}(k) - P_{pv}(k-1)}{V_{pv}(k) - V_{pv}(k-1)} \tag{13}$$

$$dE(k) = E(k) - E(k-1) \tag{14}$$

The output of the controller is the duty cycle (D) which is given by:

$$D(k) = D(k-1) + dD(k) \tag{15}$$

where $P_{pv}(k)$ and $V_{pv}(k)$ are respectively, the PV panel power and voltage at sampling instants (kTs).

$G_1$and G_2 are the gains for error and change of error respectively, and G_3 is the gain for the duty cycle variation.

Each universe of discourse of the error, change in error and duty cycle is divided into five fuzzy sets. All the membership functions are shown in Table 3 and Fig.5 give the rules of the fuzzy logic controller.

Table 3. Rule base for duty cycle.

d***E*** / ***E***	**NB**	**NS**	**ZE**	**PS**	**PB**
NB	**ZE**	**ZE**	**NS**	**NB**	**NB**
NS	**ZE**	**ZE**	**NS**	**NB**	**NB**
ZE	**ZE**	**ZE**	**ZE**	**ZE**	**PS**
PS	**PS**	**PS**	**PS**	**PB**	**PB**
PB	**PS**	**ZE**	**PS**	**NB**	**NB**

where: NB (Negative Big), NS (Negative Small), ZE (Zero), PS (Positive Small) and PB (Positive Big).

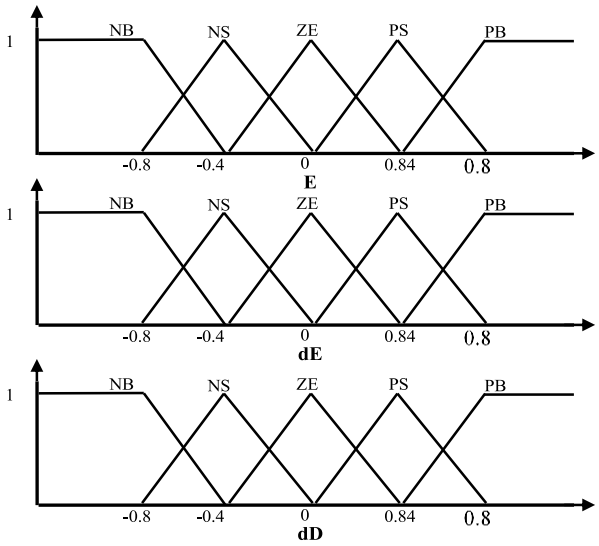

Fig. 5. Input and output membership functions of: *E*, d*E*, and d*D*.

Simulation was carried out using Sim Power System taking into account the fuzzy logic MPPT controller and boost converter. Figure 6 describes MATLAB / SIMULINK model of fuzzy based algorithm to verify the feasibility of the proposed algorithm under different climatic conditions: variable irradiance and variable temperature.

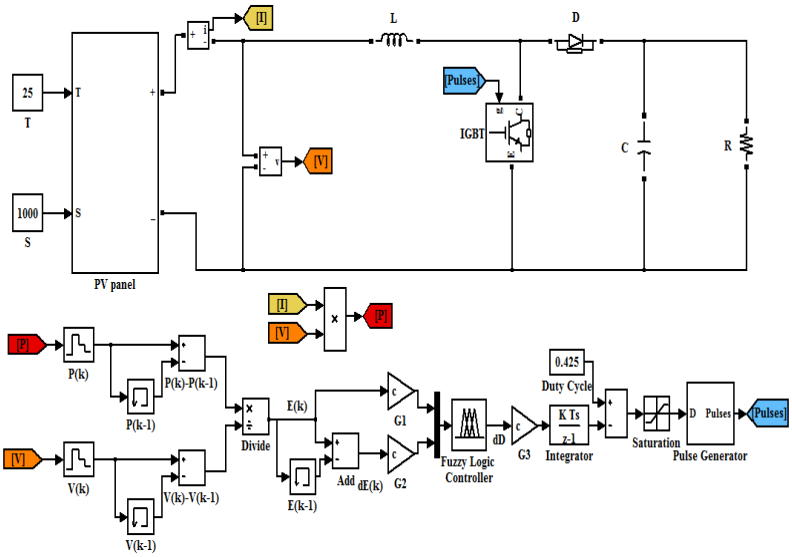

Fig. 6. MATLAB / SIMULINK model of fuzzy based algorithm.

Figure 7 shows the PV array power evolution under variable irradiance (from 400 W/m^2 to 1000W/m^2) and constant temperature (25 ° C).

Figure 8 shows the PV array power evolution under variable temperature (from 25°C to 45°C) and constant irradiance (1000 W/m^2).

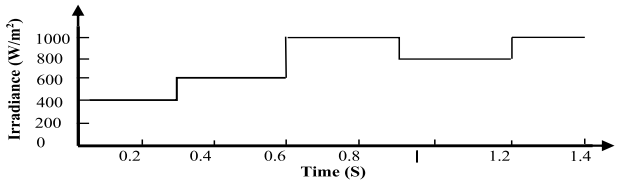

(a)

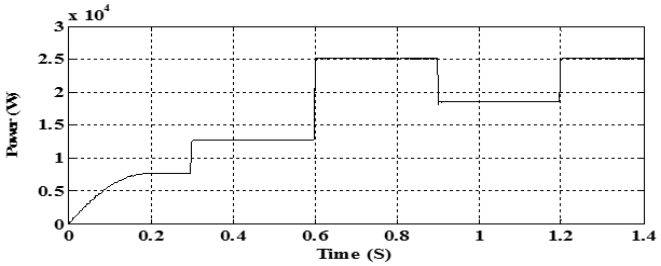

(b)

Fig. 7. PV array power evolution under variable irradiances. (a) Irradiance variation, (b) Power evolution.

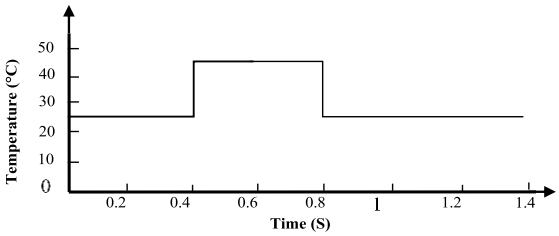

(a)

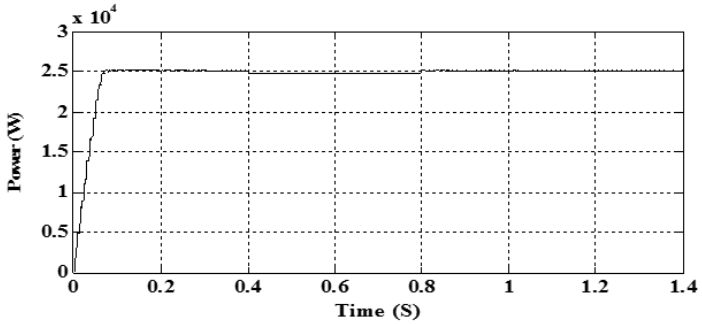

(b)

Fig. 8. PV array power evolution under variable temperatures. (a) Temperature variation, (b) Power evolution.

In Fig. 7, it is observed that fuzzy logic controller tracks the maximum power at any irradiance. As for Fig. 8, a power loss occurred when the temperature rises over the STC value.

According to Fig. 9, the input and output voltages of boost converter are shown. The corresponding boost output voltage is obtained from the input voltage at a calculated duty cycle. This output voltage will then feed the three level inverter.

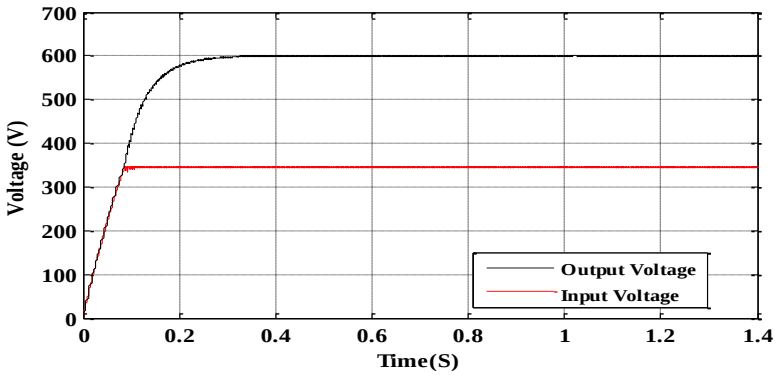

Fig. 9. Input and output voltages of DC-DC boost converter.

5. Multilevel Inverters

Two types of multilevel inverter in this paper are used: diode clamped three level inverter and modified diode clamped inverter. Multi-level inverters are used in

various applications due to their high power, low output harmonics and reduced losses [17, 18]. Description of both inverters is given in the following sections.

5.1. Diode clamped three level inverter

The diode-clamped inverter provides multiple voltage levels through connection of the phases to a series bank of capacitors. The concept can be extended to any number of levels by increasing the number of capacitors. Early description of this topology was limited to three levels where two capacitors are connected across the dc bus resulting in one additional level. The additional level was the neural point of the dc bus which was named neural point clamped (NPC) inverter. Due to capacitor voltage balancing issues, the diode clamped inverter implementation has been mostly limited to the three level inverter, which is now used extensively in industry applications.

However, a 3-level inverter requires 2 (*n*-1) switching devices, 2 (*n*-2) clamping diodes, and (*n*-1) voltage sources, *n*: number of levels. By increasing, the number of voltage levels improves the quality of the output voltage and therefore the voltage waveform becomes closer to the sinusoidal waveform.

Figure 10 shows the structure of neutral point clamped inverter in which the dc bus consists of two capacitors which allow access to potential $+V_{dc}$ /2, 0,- V_{dc}/2 [19].

The steps to synthesize the three-level voltages are summarized in Table 4, where state condition 1 means switch ON and 0 means switch OFF.

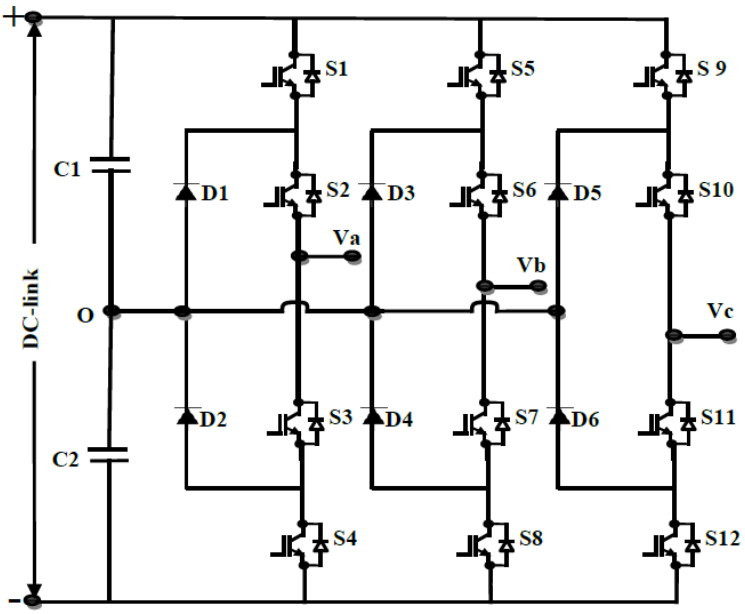

Fig. 10. Neutral point clamped inverter.

Table 4. Switching states in one leg of three-level diode clamped inverter.

Voltage, V_{ao}	S1	S2	S3	S4
$+V_{dc}/2$	1	1	0	0
0	0	1	1	0
$-V_{dc}/2$	0	0	1	1

5.2. Modified diode clamped three level inverter

The structure of the modified inverter is similar to that of the neutral point clamped diode where a capacitor is added in parallel between each of two clamping diodes for each phase. The objective of this modification is to improve the three-level inverter in terms of harmonic contents to be lower.

A one legn-level inverter requires 2(*n*-1) switching devices, 2(*n*-2) clamping diodes, (*n*-1) voltage sources , in addition to these, (*n*-2) capacitor in parallel with two clamping diodes are inserted.

Figure 11 shows the structure of modified NPC inverter topology.

6. Modulation Technique for NPC Inverter

The control signals for phase A are generated by comparing two carrier signal waves with three phase sinusoidal reference waves having fundamental frequency. The illustrated SPWM modulation technique and the control signals for the 4 power switches for phase A are exhibited as shown in Fig. 12 [20, 21]. With these control signals and by supplying both NPC inverters with a 600 V dc respectively, output voltages are produced as shown in Figs. 14 and 15.

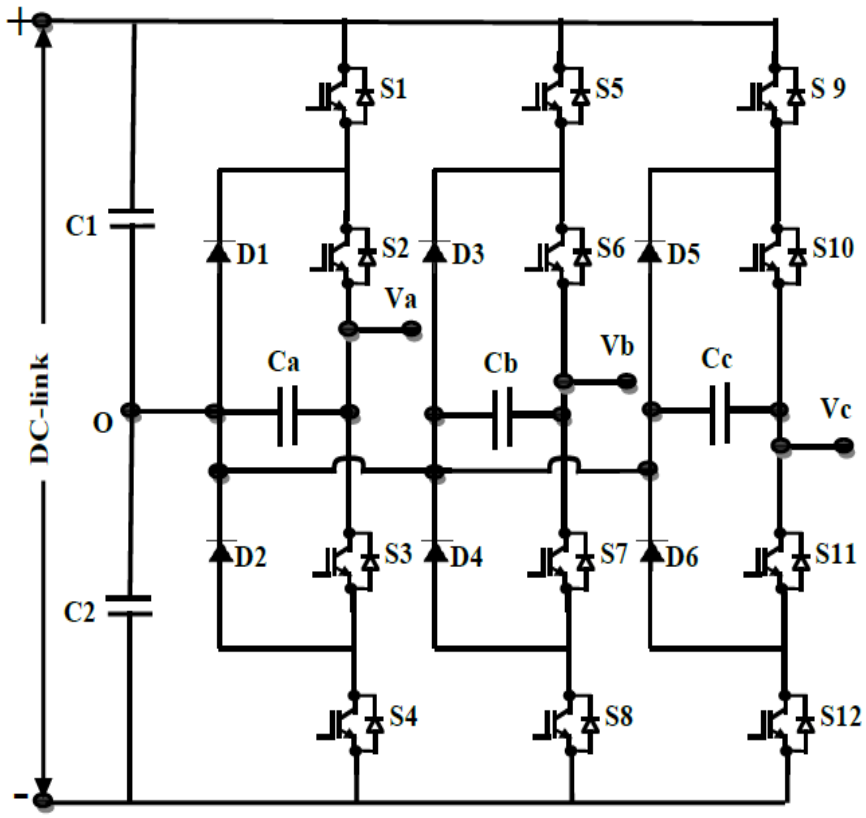

Fig. 11. Modified neutral point clamped inverter.

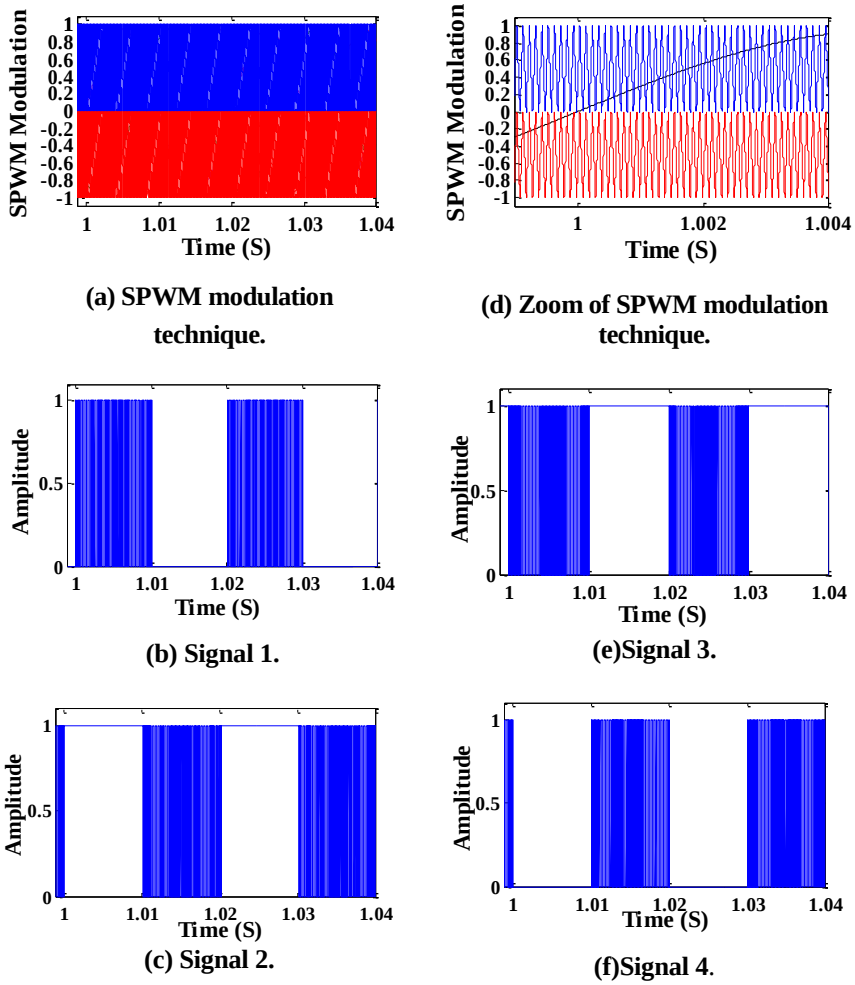

(a) SPWM modulation technique.

(d) Zoom of SPWM modulation technique.

(b) Signal 1.

(e)Signal 3.

(c) Signal 2.

(f)Signal 4.

Fig. 12. SPWM modulation technique and control signals for phase A.

7. Simulation Model and Results for the whole System

Figure 13 shows Matlab Sim power system model for the complete system used in simulation, which is carried out by feeding three-phase induction motor of squirrely cage type by first NPC inverter Fig. 14, and then modified topology inverter Fig. 15. A comparison between the two inverters is made.

Tables 5 and 6 give respectively the parameters of both NPC inverters and induction motor parameters used in simulation.

Table 5. Three level inverter parameters.

Parameter	Value
Switching frequency	10 kHz
Fundamental frequency	50 Hz
Modulation index	0.95

Table 6. Induction motor parameters.

Parameter	Value
Nominal voltage, U_n	400 V
Nominal power, P_n	4 kW
Number of poles, p	4
Stator resistance, R_s	1.405 Ω
Rotor resistance, R_r	1.395 Ω
Stator Inductance, L_s	0.005839 H
Rotor Inductance, L_s	0.005839 H
Inertia, J	0.013 kg.m^2
Mutual inductance, L_m	0.1722 H

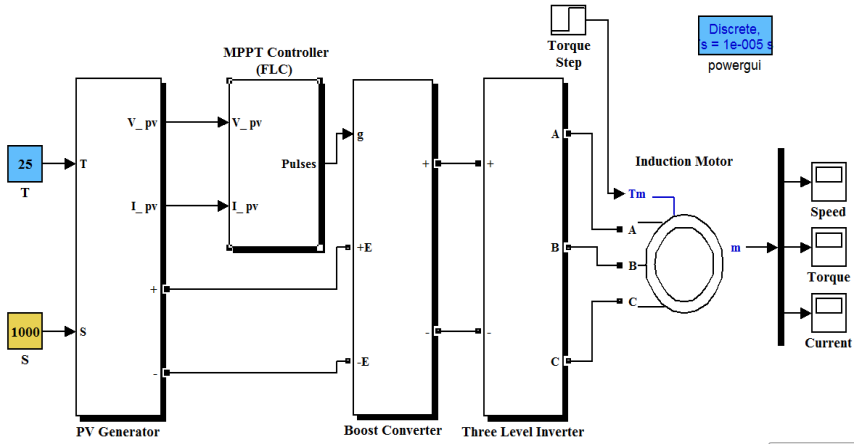

Fig. 13. Matlab Sim power system models.

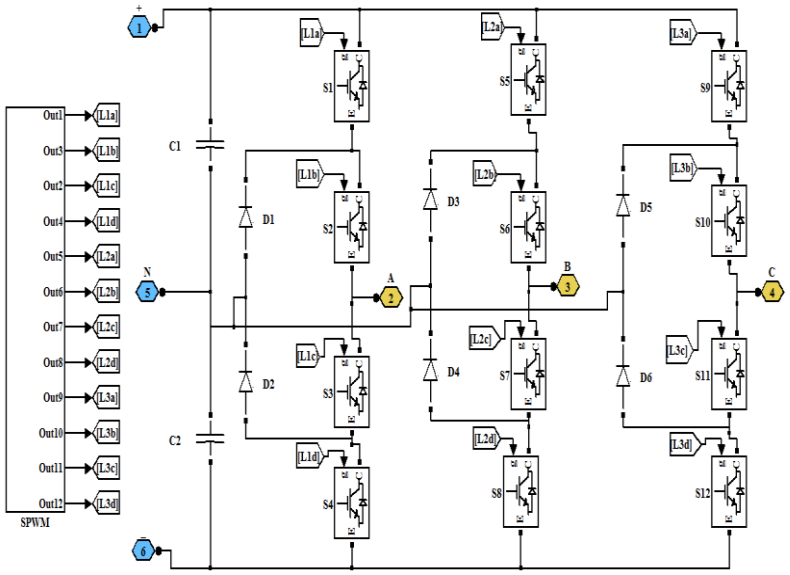

Fig. 14.Simulation circuit of neutral-point clamped inverter.

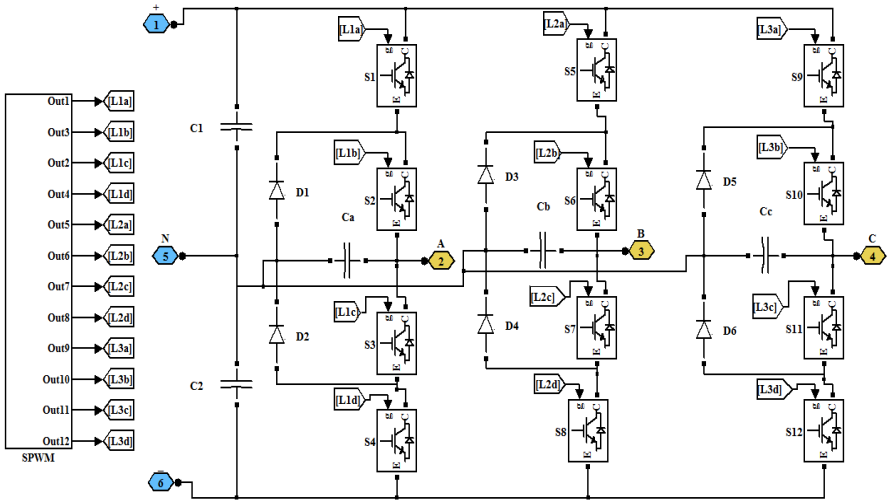

Fig. 15. Simulation circuit of modified inverter.

7.1. Results for neutral-point clamped inverter topology:

Figure 16 shows the results of the investigated shapes of neutral-point clamped inverter topology obtained by using Matlab Sim Power System.

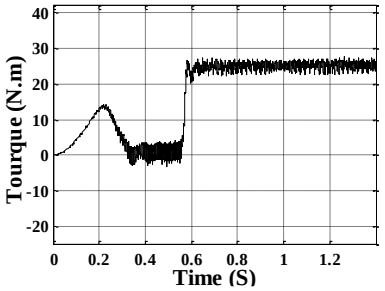

(a) The motor torque.

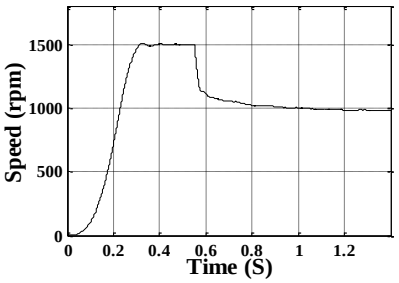

(e) The motor speed.

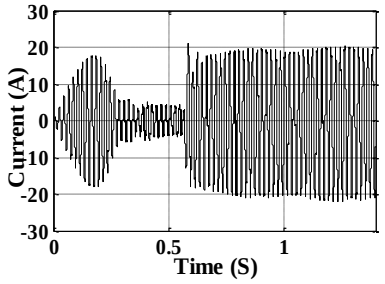

(b) The output current

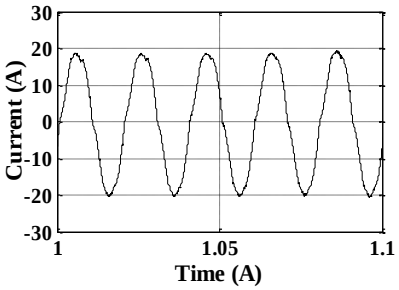

(f)The zoom of output current.

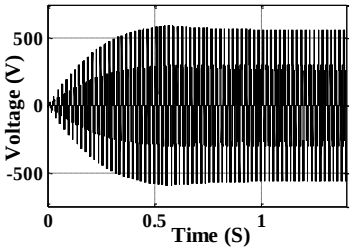

The output voltage

(c)

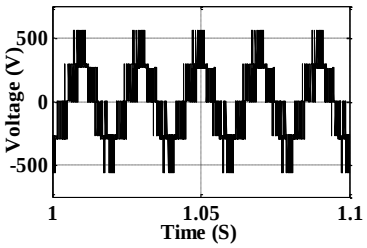

(g) The zoom of output voltage.

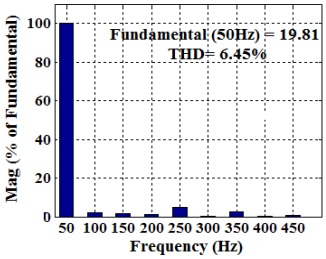

(d) FFT spectrum of the output current.

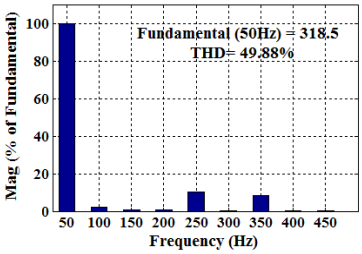

(h) FFT spectrum of the output voltage.

Fig. 16. Investigated shapes of neutral-point clamped inverter topology.

7.2. Results for modified topology

Table 7 shows the modified inverter performance when varying the capacitor value. When the capacitor increases from 3 µF to 5 µF, the current THD decreases with a rate of about 4.7 % and the voltage THD decreases with approximately 0.6%. The current THD rate of change being more important than that of the voltage. It seems that the value of 3 µF gives the best performance as shows in Figs.17 and 18 respectively.

Table 7. Modified inverter performance when varying capacitor value.

Capacitor value (uF)	THD (%) of current	THD (%) of the line to line voltage
***C* = 3µF**	5.66	47.52
***C* = 5µF**	5.94	47.24

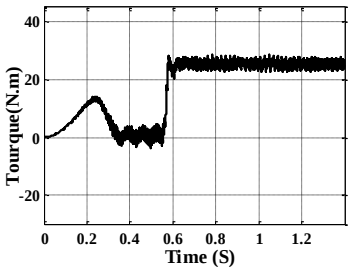

(a) The motor torque.

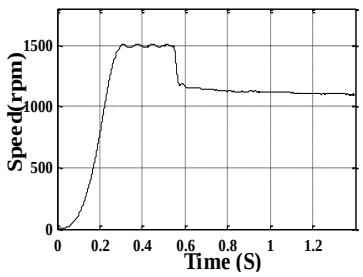

(e)The motor speed.

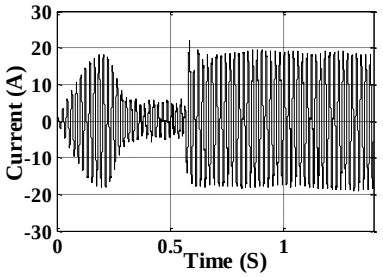

(b) The output current.

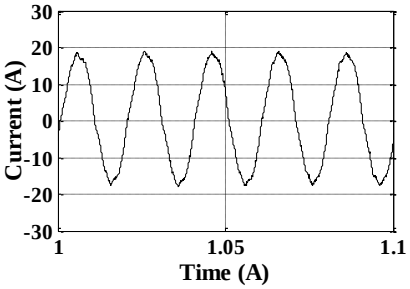

(f)The zoom of output current.

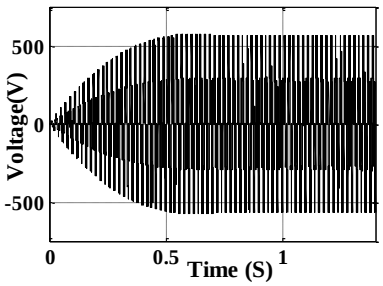

(c) The output voltage.

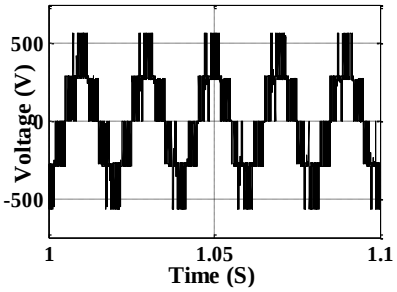

(g) The zoom of output voltage.

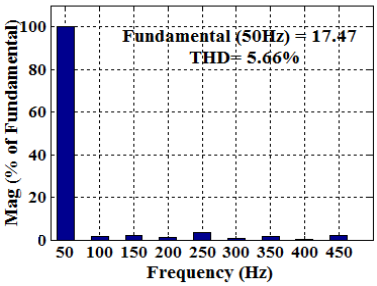

(d) FFT spectrum of the output current.

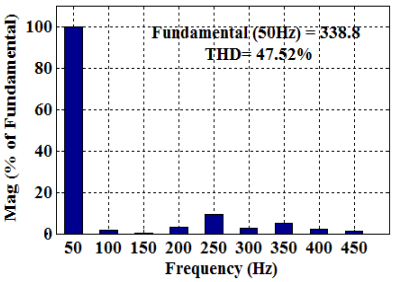

(h) FFT spectrum of the output voltage.

Fig. 17. Investigated shapes of modified topology(*C* = 3µF).

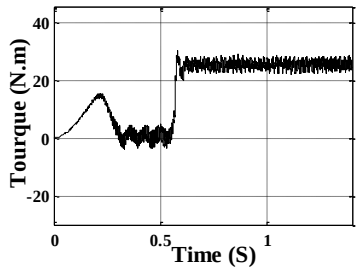

(a) The motor torque.

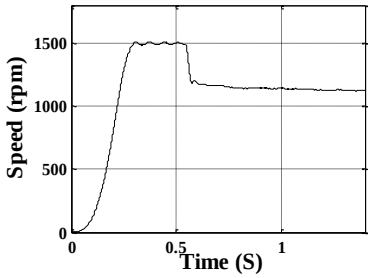

(e) The motor speed.

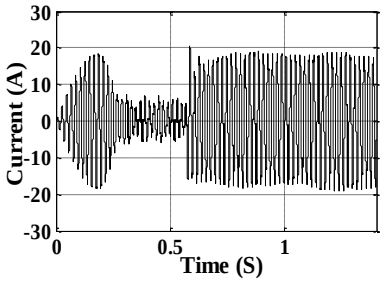

(b) The output current.

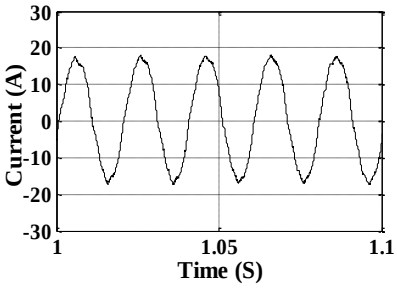

(f)The zoom of output current.

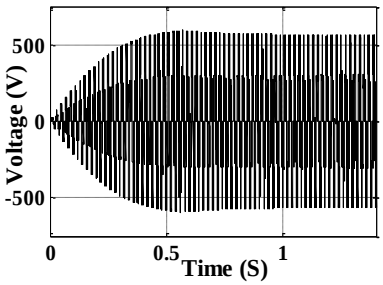

(c) The output voltage.

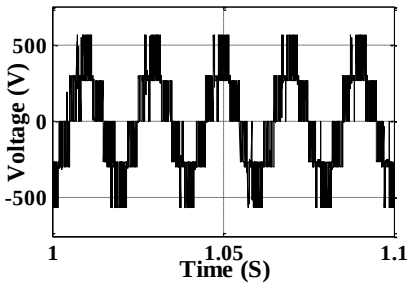

(g)The zoom of output voltage.

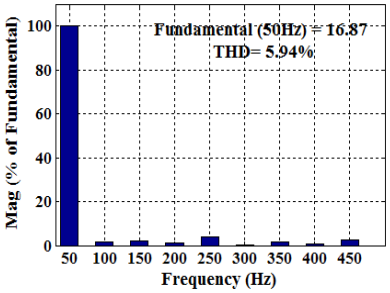

(d) FFT spectrum of the output current.

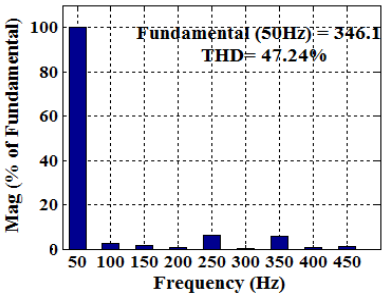

(h) FFT spectrum of the output voltage.

Fig. 18. Investigated shapes of modified topology (*C* = 5µF).

8. Results Analysis

In order to study the performance of the two topologies, Neutral-Point Clamped inverter and the modified inverter fed by PV generator, simulations were carried out using Matlab Sim Power System. The results obtained using NPC inverter are shown in Fig.16.

Figures 16(a) and (e) represent the torque and speed of induction motor respectively. The motor was started without load and at 0, 55 s a load of 25 N.m was applied. The load application resulted in a decrease in speed, which settled at approximately 988 rpm, and the torque stabilized at its nominal value.

In Figs. 16(b) and (d), the output current and its FFT spectrum are shown giving a THD of about 6.45%whereas the line to line voltage and its FFT spectrum are shown in Figs. 16(c) and (h) respectively with a THD of 49.88%and the amplitude of the fundamental of about 318.5V.

For the same simulations, the results obtained by the modified topology are shown in Figs.17 and 18 for two different values of capacitor. Figures 17(a) and (e) show the torque and speed of induction motor respectively. As previously, the motor started with no load and at 0.55s, a full load was then applied to see the performance of the system. The speed is now settled at approximately 1100 rpm and this is due to the change of fundamental voltage value from 318.5 V to 338.8 V.

Concerning the output current and its FFT spectrum shown by Figs. 17(b) and (d) respectively, it gave a THD value of about 5.66%.In Figs.17(c) and (h), the line-to-line output voltage and its FFT spectrum are shown.

It is clearly observed that a decrease in FFT spectrum compared to the conventional inverter is obtained, either in output spectrum current or in the line-to-line spectrum voltage by using capacitor of 3µF or 5µF.Table 8 summarizes the results of both inverters: NPC inverter and the modified inverter.

Table 8. Comparison between two inverter topologies.

	NPC inverter	**Modified inverter**
THD (%) of current	6.45	5.66
THD (%) of line to line voltage	49.88	47.52
Fundamental, V	318.5	338.8
Speed, rpm	988	1100

9. Conclusions

In this paper, two types of multilevel inverter are used: diode clamped three level inverter and modified diode clamped inverters, which are fed by PV system as DC source input to drive an induction motor. The circuit topology, modulation technique and operational principle of the proposed inverter were analysed in detail. A MPPT fuzzy logiccontroller is implemented to continuously adjust the PV output power to its maximum value, which is mostly related to the changes in atmospheric conditions.

The simulations were carried out using Sim Power System. According to the simulation results, which are summarized in Table 8, the modified inverter has clearly shown better performances compared to the conventional inverter in terms of THD of current and line-to-line voltage. Furthermore, the proposed modified inverter is more efficient and generates less harmonic content so the improvement of quality power will be then achieved.

Nomenclatures

G	Irradiance
G_{raf}	Irradiance at standard test conditions (STC)
I	Photovoltaic output current, A
I_{ph}	Light generated current in a PV module, A

I_o	Diode saturation current, A
k	Boltzmann constant (=1.3806503×10^{-23} J/K)
n	Ideality factor temperature
q	Electron charge(=1.60217646×10^{-19} C)
R_s	Series resistance of a PV module, Ω
R_{sh}	Intrinsic shunt resistance of the cell, Ω
T	Temperature condition of work, ^{o}C
V	Photovoltaic output voltage, V
V_T	The thermal voltage, V

Greek Symbols

μ_{icc}	Coefficient temperature of short circuit current, A/K

Abbreviations

FFT	Fast Fourier Transform
MPPT	Maximum Power Point Tracking
NPC	Neutral-Point Clamped Diode Inverter
SPWM	Sinusoidal Pulse Width Modulation
STC	Standard Test Conditions
THD	Total Harmonic Distortion

References

1. El-Fergany, A. (2015).Efficient tool to characterize photovoltaic generating systems using mine blast algorithm. *Electric Power Components and Systems*, 43(8-10), 890-901.
2. Abouda, S.; Nollet, F.; Chaari, A.; Essounbouli, N.; and Koubaa, Y. (2013). Direct torque control - DTC of induction motor used for piloting a centrifugal pump supplied by a photovoltaic generator. *International Journal of Electrical, Computer, Energetic, Electronic and Communication Engineering*, 7(8), 1110-1115.
3. Abdourrziq, M.; Ouassaid, M.; and Maaroufi, M. (2016).Single-sensor based MPPT for photovoltaic systems. *International Journal of Renewable Energy Research*, 6(2), 570-579.
4. Sridhar, S.; Raj, P.G.; Ramaprabha, R.; and Muthu, R. (2008). Microcontroller based maximum power point tracking control for PV fed space vector controlled three phase induction motor. *In TENCON 2008-2008 IEEE Region 10 Conference*, 1-4.
5. Lee, J.-S.; Lee, S.-J.; and Lee, K.-B. (2018). Novel switching method for single-phase NPC three-level inverter with neutral-point voltage control. *International Journal of Electronics*, 105(2), 303-323.
6. Sruthi, C.K.; and Saritha, P. (2014). A novel multilevel inverter using single carrier PWM technique. *In 2014 International Conference on Circuit, Power and Computing Technologies (ICCPCT)*, 468-472.
7. Kim, S.-H.; and Kim, Y.-H. (2008). Design and analysis of an LC trap/LCR output filter for a single-phase NPC three-level inverter. *International Journal of Electronics*, 95(12), 1279-1292.
8. Bakhshizadeh, M.K.; Iman-Eini, H.; and Blaabjerg, F. (2015). Selective harmonic elimination in asymmetric cascaded multilevel inverters using a new

low-frequency strategy for photovoltaic applications. *Electric Power Components and Systems*, 43(8-10), 964-969.

9. Albert, A.S.; and Manigandan, T. (2014). Digital control strategy for solar photovoltaic fed inverter to improve power quality. *Journal of Renewable and Sustainable Energy*, 6(1), 013128.
10. Adam, G.P.; Anaya-Lara, O.; Burt, G.; Finney, S.J.; and Williams, B.W. (2009). Comparison between flying capacitor and modular multilevel inverters. *In 35th Annual Conference of the IEEE Industrial Electronics Society-IECON Porto, Portugal*, 271-276.
11. Habbati, B.; Ramdani, Y.; and Moulay, F. (2014).A detailed modeling of photovoltaic module using MATLAB. *NRIAG Journal of Astronomy and Geophysics*, 3(1), 53-61.
12. Nowdeh, S.A.; Ghahnavieh, A.R.; and Shojaei, H. (2012). Reliable Designing of Stand-alone PV/FC Hybrid System. *Majlesi Journal of Electrical Engineering*, 7(2), 41-47.
13. Alsumiri, M.A.; Jiang, L.; and Tang, W.H. (2014). Maximum power point tracking controller for photovoltaic system using sliding mode control. In *Proceedings of the 3rd IEEE onRenewable Power Generation Conference*, Naples, Italy, 7-3.
14. Masri, S.; and Chan, P.W. (2010). Design and development of a dc-dc Boost converter with constant output voltage. *In Intelligent and Advanced Systems (ICIAS), International Conference on (pp. 1-4). IEEE.*
15. Sudhakar, N.; Rajasekar, N.; Akhil, S.; and Reddy, K.J. (2017). Chaos control in solar fed DC-DC boost converter by optimal parameters using nelder-mead algorithm powered enhanced BFOA. In *Proceedings of IOP Conference Series: Materials Science and Engineering*, 263, 1-22.
16. Dib, A. (2016). Predictive direct power control of a grid connected three-phase voltage source inverter for photovoltaic systems. *International Journal of Renewable Energy Research (IJRER)*, 6(1), 212-219.
17. Singh, P.; Palwalia, D.; Gupta, A.; and Kumar, P. (2015).Comparison of photovoltaic array maximum power point tracking techniques. *International Advanced Research Journal in Science, Engineering and Technology*, 2(1), 401-404.
18. Mittal, N.; Singh, B.; Singh, S.P.; Dixit, R.; and Kumar, D. (2012). Multilevel inverter: A literature survey on topologies and control strategies. In *Proceedings of 2nd International Conference on Power, Control, Embedded Systems*, 1-11.
19. Tayab, U.B.; and Al-Humayun, M.A. (2017). Operation and control of cascaded h-bridge multilevel inverter with proposed switching angle arrangement techniques. *Journal of Engineering Science and Technology*, 12(12), 3148-3157.
20. Budi, S.R.; and Sharma, S. (2014). A novel method of nine level inverter fed induction motor drive. In *Proceedings of 2014 International Conference on Advances in Engineering and Technology Research (ICAETR)*, 1-4.
21. Pathak, S.M.; and Satarkar, M.F.A.R. (2017).Three level active neutral point clamped inverter with sinusoidal PWM control.*International Journal of Current Engineering and Scientific Research* (*IJCESR*), 4(7), 26-29.